

Growth and optical properties of $\text{CdS}_x\text{Se}_{1-x}$ nanocrystals embedded in a novel phosphate glass

A. A. LIPOVSKII, E. V. KOLOBKOVA, V. D. PETRIKOV
St.-Petersburg State Technical University, Polytechnicheskaja 29,
St.-Petersburg, 195251 Russia
E-mail: lipovskii@phtf.stu.neva.ru

A novel high optical quality phosphate glass embedded with nanocrystals of $\text{CdS}_x\text{Se}_{1-x}$ ($x = 0, 0.4, 0.5, 0.7, 0.8, 1.0$) has been synthesised and studied. Thermal processing of the glass varies both size and size distribution of the nanocrystals. Complicated structure of optical absorption spectra of the glass samples is demonstrated. © 1999 Kluwer Academic Publishers

1. Introduction

First studies of glasses embedded with semiconductor nanocrystals (semiconductor doped glasses) demonstrated quantum confinement of electronic excitations in the semiconductor grains: blue shift of optical absorption edge and discrete structure of electron-hole transitions [1, 2]. Later both experimental and theoretical studies of energy structure of the nanocrystals [3–12] and the studies of their growth [13–18] were performed. The semiconductor doped glasses (SDGs) are convenient for basic studies of quantum size phenomena, and the usage of SDG in dynamic holography [19, 20], for lasing [21] and for second harmonic generation [22] has also been demonstrated. Commercial silicate SDG (colour filters) of high optical quality and highly concentrated nanocrystalline doped samples made with chemical techniques [8, 11] have been used in the experiments. The chemical techniques provide extremely low size-dispersive semiconductor nanocrystals, but these techniques are hardly useful for producing bulky samples of high optical quality, which could be suitable for applications. From the other side, SDG synthesised with conventional techniques (colour filters) can not contain more than ~0.1 wt % of II–VI semiconductors due to poor solubility of the semiconductors in conventional silicate glass matrices, and size distribution of semiconductor nanocrystals embedded in the commercial glasses is usually wide (about 50%). Low concentration and wide size distribution of the nanocrystals in the silicate glasses restrict their applicability, e.g., in non-linear optics. Silicate glass colour filters are also poorly suitable for studies of quantum transitions in embedded nanocrystals due to wide size distribution of the crystallites, and nanocrystalline-doped samples prepared with other techniques, for example, colloidal samples [8], are mainly used for these studies. Conventional silicate SDGs have to be annealed for tens of hours above glass transition temperature (600–650 °C) for growing the semiconductor

crystallites, and these conditions of thermal treatment are hard. Therefore, design of a highly concentrated nanocrystalline-doped material, which is suitable both for fundamental studies and for applications, is of importance. As far as we can judge, the only material, which has higher concentration and narrower dimensional distribution of semiconductor nanocrystals and can compete in optical quality of bulky samples with silicate SDG, is a novel phosphate SDG presented in our previous paper [23]. In this paper we report formation and growth of Cd-S-Se nanocrystals in the phosphate glass.

2. Phosphate glass annealing and optical absorption edge

We used $\text{P}_2\text{O}_5\text{-Na}_2\text{O-ZnO-AlF}_3\text{-Ga}_2\text{O}_3$ glass system doped with Cd-S-Se ternary semiconductor. The phosphate glass system is more flexible comparatively to conventional silicate glass systems, and it is suitable for doping with the semiconductors in increased concentration [23]. Composition of the glass was presented in our previous paper [23], but percentage of gallium was increased for higher transition temperature T_G and better chemical stability of the glass. Measured concentration and composition of II–VI semiconductor for different series of glass samples are presented in Table I, maximal concentration is equal to 1.2 wt % for $\text{CdS}_{0.73}\text{Se}_{0.27}$ dopant. This is about 1.5 order of magnitude higher comparatively to conventional silicate SDG.

Annealing of the glass samples at 400–440 °C induces their colouring from light yellow to dark red. The colouring depends on the temperature and on the duration of the annealing, on dopant composition and concentration. This behaviour is similar to the behaviour of conventional silicate SDG, and it is the same way influenced by quantum confinement phenomena in II–VI semiconductor nanocrystals embedded in the glass. However, the conditions of the annealing

TABLE I Composition x and concentration of II–VI semiconductors in different series of the phosphate glass samples doped with $\text{CdS}_x\text{Se}_{1-x}$

Series of samples	A	B	C	D	E	F
Composition parameter x	1	0.754	0.725	0.475	0.409	0
Semiconductor concentration (wt %)	1.055	0.975	1.22	0.685	0.745	0.655

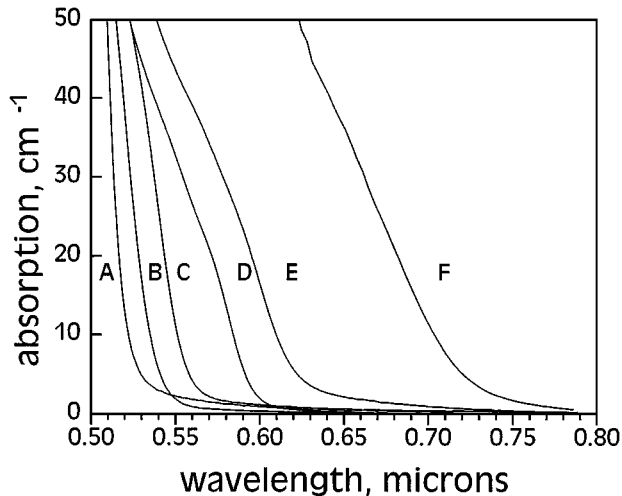


Figure 1 Absorption spectra of $\text{CdS}_x\text{Se}_{1-x}$ doped phosphate glass for A–F series samples annealed at 410°C : A, B, D, E – 90 min, C – 45 min, F – 5 min.

of the phosphate SDG are much softer comparatively to silicate SDGs: the temperature of the processing ($420\text{--}440^\circ\text{C}$) is lower, and the annealing is shorter (several minutes and tens of minutes instead of several tens of hours for silicate glasses). This is due to low viscosity and fast diffusion of the semiconductor in the glass at the annealing temperature.

Transmission electron microscopy of the annealed phosphate SDG shows existence of nanograins embedded in the glass matrix, and X-ray diffractometry of the glass samples (series E) shows reflection peaks indicating hexagonal crystalline structure of these grains. Positions of the peaks are in coincidence with semiconductor composition. Optical absorption spectra of the glass samples of different seria are presented in Fig. 1 (mainly long time annealing at 410°C : series A, B, D, E samples (90 min); C sample (45 min); F sample (5 min); and Se concentration in the F sample slightly differs with data presented in Table I). The variety of dopant composition and annealing duration makes possible the positioning of optical absorption edge of the phosphate SDG within spectral range $400\text{--}700\text{ nm}$.

3. Growth of nanocrystals

Optical absorption spectroscopy of differently annealed phosphate glass samples indicated several stages of the growth of the nanocrystals. To characterise the processes of growth we used the position of the first absorption maxima (formed by transition between the highest hole and the lowest electron states) in differently annealed samples for estimating average size of

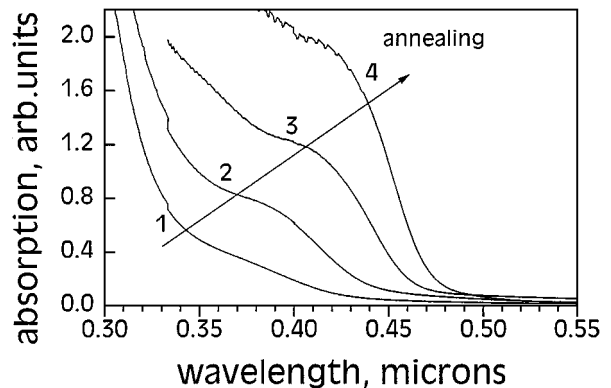


Figure 2 Transformation of absorption spectra of the phosphate glass samples (E-series) under short-time annealing at 410°C : (1) 5 min, (2) 5 + 3 min, (3) 5 + 4 min, (4) 5 + 5 min.

the nanocrystals. For CdSe-doped glass one can use experimentally observed HOMO-LUMO (high obtained molecular orbital – low unobtained molecular orbital) gap as the function of the particle size [6]. For CdS and Cd-S-Se nanocrystals we used simple effective mass approximation under Coulomb interaction, the model was corrected according to known relation of theoretical predictions and experimental results for CdSe [6]. We suppose this approach can be used for first order estimation illustrating the growth of the nanocrystals. For mixed compositions we used linear relations to calculate band gap and effective mass (at 300 K for pure CdSe $E_g = 1.74\text{ eV}$, $m_e^* = 0.11m_0$, for CdS $E_g = 2.53\text{ eV}$, $m_e^* = 0.17m_0$). Certainly, for correct evaluation of the size the change of the nanocrystals' composition at initial stages of the growth [24] should be accounted. This needs additional X-ray diffraction and Raman scattering measurements.

The transformation of the optical absorption spectra of the nanocrystals at initial stages of the growth is illustrated with Fig. 2, where the spectra of the samples annealed at 410°C (initially 5 min, and then additionally 3, 4 and 5 min) are presented. Evaluated average radius of the nanocrystals is increasing in the range $\sim 0.8\text{--}1.0\text{ nm}$ due to the additional annealing. This means that the crystallites are practically equal during first 5–10 min of the annealing, and the heat treatment leads mainly to the increase of the absorption. This stage can be treated as nucleation (the nuclei are practically monodisperse, and the increase of optical absorption is due to increasing number of the nuclei). High concentration of the semiconductor dopant in the phosphate SDG leads to the formation of great number of the nuclei with the first peak of optical absorption laying in the region of the transparency of the glass matrix, and optical absorption of the nuclei is easily observable with standard techniques.

At the second stage of the growth all nuclei independently increase their size until the oversaturation of the solid solution of the semiconductor in the glass become negligible. This process is illustrated with Fig. 3, where transformation of the glass optical absorption spectrum (E-series of samples) under annealing up to 30 min at 415°C is shown. The spectra of shortly annealed glass samples (nuclei formation stage) look similarly, but in

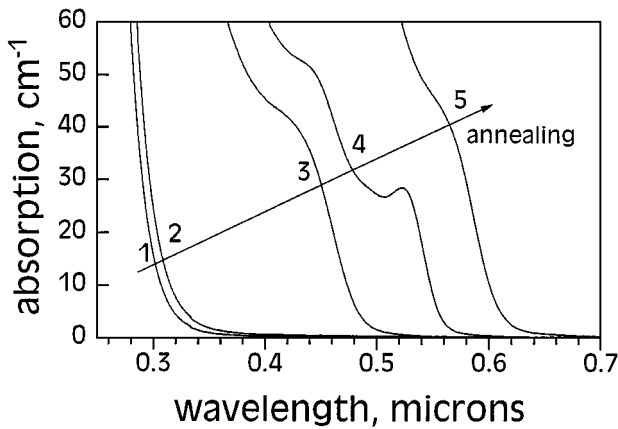


Figure 3 Transformation of optical absorption spectra of the phosphate glass samples (E-series) annealed at 415 °C: (1) 0 min, (2) 5 min, (4) 10 min, (5) 30 min, (3) 300 min at 395 °C.

10 min the diffusive growth of nuclei begins. At this stage the shift of the first optical absorption peak occurs, and the absorption spectrum becomes well structured due to electron-hole transitions in the semiconductor nanocrystals. The annealing up to 30 min induces further shift of optical absorption edge and smoothing the spectrum. Average radius estimated for 5 min annealing is ~ 0.8 nm, after 10 min it becomes ~ 2.3 nm, and in 30 min ~ 3.8 nm. In Fig. 3 we also show the spectrum of the sample annealed at lower temperature (300 min, 395 °C, average radius ~ 1.2 nm). Lower growth rate and longer thermal processing lead to the formation of increased number of the nuclei comparatively to the annealing at 415 °C, and the absorption peak corresponding to the first optical transition is higher. For longer annealing the oversaturation of the solid solution drops, and growth of the nanocrystals under mutual influence replaces their independent diffusive growth. This final stage of the growth is coalescence [25]. The concentration of semiconductor in silicate SDGs is low, and oversaturation drops when the transformation of absorption spectra is negligible comparatively to unannealed glass [1, 2]. Due to this reason the first and the second stages of the nanocrystals' growth in silicate glasses and the complicated structure of optical absorption were observed only last years [13]. High concentration of II–VI semiconductor in the designed phosphate SDG causes the prolongation of the first and the second stages of the growth, and these stages are observed in our experiments.*

4. Confined energy spectrum and size distribution of the crystallites

High concentration of the semiconductor in the phosphate SDG leads to the formation of numerous nuclei with narrow size distribution (nucleation stage [13]), Fig. 2. Then due to high concentration of the

* As for coalescence, high concentration of semiconductor and related high rate of growth of the nanocrystals in the glass leads to positioning of the grains' optical absorption edge close to absorption edge of bulk semiconductors by the end of the second stage of the growth, and coalescence stage was difficult to observe with optical techniques unless the concentration was decreased.

semiconductor dopant in the glass diffusive growth of the grains increases size of nuclei practically without change of the initial size distribution. Therefore glass samples with well-structured absorption spectrum can be easily formed. Optical absorption spectra ($T = 300$ K) of CdSe and CdS doped phosphate SDG, respectively, are presented in Fig. 4. The estimated average radius is ~ 2.8 nm for CdSe and ~ 2.3 nm for CdS nanocrystals. Since radius of the nuclei does not exceed exciton radius for both semiconductors, we observe transitions from hole quantum states to electronic ones [5]. Absorption spectrum of CdS-doped sample demonstrates complicated structure similarly to the spectra of colloidal CdSe samples [6]. As far as we know, this is the most complicated spectral structure observed in CdS doped bulk glasses up to now. Spectral measurements at liquid nitrogen temperature (80 K) show additional blue shift of the transitions (approximately 60 meV for the first excited state) and reduced thermal broadening of the absorption peaks, but the structure of the spectra is the same. To illustrate positions of the absorption peaks second derivatives of the spectra are also plotted in Fig. 4, and the positions of the absorption lines are presented in Table II. Similarly structured spectra were also observed for the samples of B-D seria. The spectra of optical absorption show that size distribution of the nanocrystals is narrow. We used known size-dependence of the position of the first optical transition [6, 8] to evaluate the width of the size distribution from the width of the first peak of

TABLE II Positions of the minima of second derivatives of the absorption spectra of CdS and CdSe nanocrystals embedded in the phosphate glass

Peak positions (eV)	Peak number					
	1	2	3	4	5	6
CdSe	2.01	2.12	2.30	2.47	2.86	3.3
CdS	2.69	2.82	2.96	3.22	3.55	3.9

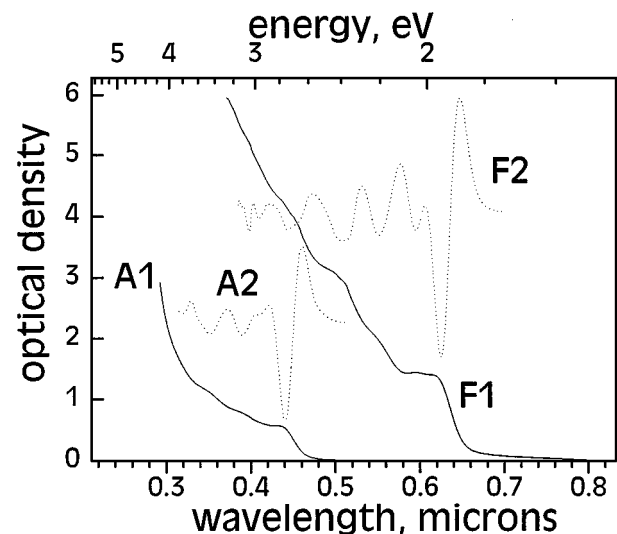


Figure 4 Optical density spectra (A1, F1) and second derivatives (A2, F2) of the spectra of CdS doped phosphate glass (A-series, 5 min annealing at 390 °C) and CdSe doped phosphate glass (F-series, 15 min annealing at 410 °C).

optical absorption measured at liquid nitrogen temperature. Evaluated width does not exceed 15–20%, while for coalescent growth the width is ~50% [25]. This proves that coalescence does not occur at the experimental situation, and this is due to high concentration of the semiconductor in the glass.

5. Conclusions

Finally the novel high optical quality phosphate glass doped with increased concentration of Cd-S-Se nanocrystals was designed. Annealing of the glass provides positioning optical absorption edge within the spectral range 400–700 nm. Different stages of the growth of the nanocrystals were observed. High concentration of the semiconductor dopants allowed us to observe the peak of optical absorption of nuclei with radii down to ~1 nm. Influence of the annealing conditions on the formation of the nuclei was examined. The phosphate SDG samples with narrow size distribution of the nanocrystals were formed, and a complicated structure of the optical absorption spectra has been observed for the glass doped with Cd-S-Se alloys of different composition.

Acknowledgements

The research has been supported by Russian National Program “Physics of Solid Nanostructures (FTNS)”.

References

1. A. I. EKIMOV and A. A. ONUSHCHENKO, *Sov.-Phys. Semicond.* **16** (1982) 775.
2. R. ROSSETTI, S. NAKAHARA and L. E. BRUS, *J. Chem. Phys.* **79** (1983) 1086.
3. AL. L. EFROS and A. L. EFROS, *Sov.-Phys. Semicond.* **16** (1982) 772.
4. AL. L. EFROS and A. V. RODINA, *Phys. Rev. B* **15** (1993) 10005.
5. A. I. EKIMOV, F. HACHE, M. C. SCHANNE-KLEIN, D. RICARD, C. FLYTZANIS, I. A. KUDRYAVTSEV, T. V. YAZEVA and A. V. RODINA, *J. Opt. Soc. Amer. B* **10** (1993) 100.
6. C. B. MURRAY, D. J. NORRIS and M. G. BAWENDI, *J. Amer. Chem. Soc.* **115** (1993) 8706.
7. D. J. NORRIS, A. SACRA, C. B. MURREY and M. G. BAWENDI, *Phys. Rev. Lett.* **72** (1994) 2612.
8. D. J. NORRIS and M. G. BAWENDI, *Phys. Rev. B* **53** (1996) 16338.
9. K. L. STOKES, H. YUKSEICI and P. D. PERSANS, *Solid State Commun.* **92** (1994) 195.
10. P. A. M. RODRIGES, G. TAMILAITIS, P. Y. YU and S. H. RISBUD, *ibid.* **94** (1995) 583.
11. W. HOHEISEL, V. L. COLVIN, C. S. JOHNSON and A. P. ALIVISITOS, *J. Chem. Phys.* **101** (1994) 8455.
12. P. LEFEBVRE, T. RICHARD, J. A. ALLEGRE, H. MATHEIEU, A. PRADEL, J.-L. MARK, L. BOUDES, W. GARNIER and M. RIBES, *Superlattices and Microstructures* **15** (1994) 447.
13. S. A. GUREVICH, A. I. EKIMOV, I. A. KUDRYAVTSEV, O. G. LUBLINSKAYA, A. V. OSINSKII, A. S. USIKOV and N. N. FALEEY, *Semiconductors* **28** (1994) 486.
14. A. I. EKIMOV, *Physica Scripta* **39** (1991) 217.
15. V. ESCH, G. FLUEGEL, G. KHITROVA, H. M. GIBBS, XU JIAJIN, K. KANG, S. W. KOCH, L. C. LIU, S. H. RISBUD and N. PEYGHAMBARIAN, *Phys. Rev. B* **42** (1990) 7450.
16. L.-C. LIU and S. H. RISBUD, *J. Appl. Phys.* **68** (1990) 28.
17. M. P. A. MUELLER, U. LEMBKE, U. WAGGON and I. RUECKMANN, *J. Non-Cryst. Solids* **144** (1992) 240.
18. W. S. O. RODDEN, C. N. IRONSIDE and C. M. SOTOMAYOR TORRES, *Semicond. Sci. Technol.* **9** (1994) 1839.
19. R. K. JAIN and R. C. LIND, *J. Opt. Soc. Amer.* **73** (1983) 647.
20. S. M. SALTIEL, B. VAN WONTERGHEM, P. A. PARTENOPOULOS and T. E. DUTTO, *Appl. Phys. Lett.* **54** (1989) 1842.
21. V. S. DNEPROVSKII, V. I. KLIMOV, D. K. OKOROKOV and YU. V. VANDYSHEV, *Phys. Status Solidi (b)* **173** (1992) 4056.
22. N. M. LAWANDY and R. L. MACDONALD, *J. Opt. Soc. Amer. B* **8** (1991) 1307; N. M. LAWANDY and J. KYUNG, *Laser Focus World* **32** (1996) 131.
23. E. V. KOLOBKOVA, A. A. LIPOVSKII, N. V. NIKONOROV and A. A. SITNIKOVA, *Phys. Status Solidi (a)* **147** (1995) K65.
24. A. RAMOS, O. LYON and C. LEVELUT, *J. Appl. Phys.* **78** (1995) 6916.
25. E. M. LIFSHITZ and L. P. PITAEVSKII, “Physical Kinetics” (Pergamon Press, New York, 1981) p. 432.

Received 27 November 1996
and accepted 7 October 1998